

Statistical analysis and modeling of variance in the SA-I mechanoreceptor response to sustained indentation

Daine R. Lesniak, *Student Member, IEEE*, Scott A. Wellnitz, Gregory J. Gerling*, *Member, IEEE*, and Ellen A. Lumpkin

Abstract— The slowly-adapting type I mechanoreceptor (SA-I) exhibits variability in its steady-state firing rate both within an afferent upon repeated stimulation and between afferents. Additionally, inter-spike intervals of the SA-I are extremely variable during this steady-state firing. While variability of the SA-I response has been noted previously, the work presented herein provides a finer analysis of the impact of force and fiber on the SA-I response. Specifically, we test two hypotheses, that 1) fiber-to-fiber variation will significantly impact firing rate over the range of applied forces, and that 2) fiber-to-fiber variation will significantly impact the coefficient of variation (CV) of inter-spike intervals over the range of applied forces. Utilizing an *ex vivo* skin nerve preparation in the mouse, experiments were conducted with six SA-I fibers from five mice, and with compressive stimuli with force magnitudes up to 9.59 mN. We found fiber to significantly impact both firing rate and CV. These findings motivated the construction of a generalized input (force) – output (firing rate) model composed of a baseline response profile and a multiplicative fiber sensitivity factor. This work will inform future efforts to attribute variability to differences in skin, neuron, and receptor properties, and will contribute to the understanding of how much variability is acceptable in systems designed to provide tactile feedback to the nervous system.

I. INTRODUCTION

The slowly adapting type I (SA-I) mechanoreceptor is characterized by high spatial acuity to edges and curvature, responses over a range of frequencies, and slow adaptation in spike firing elicited by static indentation [1-3]. SA-Is are found in both hairy and glabrous skin of vertebrates, including primates [4, 5] and mice [6]. The end

Manuscript received April 7, 2009. This work was supported by grants from the Defense Advanced Research Projects Agency (DARPA grant to GJG), the National Library of Medicine (Grant Number T15LM009462 to GJG) and the NIH (NIAMS R01 AR051219 to EAL). The content is solely the responsibility of the authors and does not necessarily represent the official views of DARPA, the National Library of Medicine, or the National Institutes of Health.

D. R. Lesniak is with the Department of Systems and Information Engineering, University of Virginia, Charlottesville, VA 22904 USA. (e-mail: drl2v@virginia.edu).

*Correspondence to G. J. Gerling, Department of Systems and Information Engineering, University of Virginia, Charlottesville, VA 22904 USA. (phone: 434-924-0533; fax: 434-982-2972; e-mail: gregory-gerling@virginia.edu).

S. A. Wellnitz is with the Department of Neuroscience, Baylor College of Medicine, Houston, TX 77030 USA. (e-mail: wellnitz@bcm.edu).

E. A. Lumpkin is with the Departments of Neuroscience, Molecular Physiology & Biophysics, and Molecular & Human Genetics, Baylor College of Medicine, Houston, TX 77030 USA. (e-mail: lumpkin@bcm.edu).

organ associated with the SA-I afferent is the Merkel cell-neurite complex (MCNC). The MCNC features a tree-like cluster of a few to dozens of Merkel cells (dependent on species and body site) [6, 7] and is located in the basal layer of the epidermis, near the dermis [8].

The SA-I exhibits an unusually high variance of inter-spike intervals in response to sustained mechanical stimuli in the steady state. Variability is also observable i) within a fiber to repeated stimulation, and ii) between fibers to like stimuli. These aspects of variability have been investigated by a number of researchers following the initial work of Iggo and Muir [2]. For example, Knibestol noted the varied degree of SA-I discharge to levels of skin displacement and velocity [9]. Others have noted variability in the generation of impulses and discussed its potential causes [10, 11] and attempted to take factors such as fiber sensitivity, noise, and covariance into account in modeling SA-I populations [12, 13].

For more than a century, researchers have sought to understand the SA-I response through experiments involving vibratory [14], white noise [15], and sustained stimuli [1, 12, 13, 16]. While these efforts have greatly increased our understanding of how the SA-I afferent converts skin deformation into a neural response and how the highly variable responses from a population of receptors are interpreted by the brain [17], many details have yet to be resolved. For example, the various types of SA-I variability have yet to be assigned physiological sources. Some of the variability may be due to differences in the skin, neuron, or end organ. To augment prior work, this work investigates the impact of fiber on sustained SA-I responses elicited by sustained stimuli in the mouse, a genetically tractable mammal. Additionally, this work examines a generalized model of the SA-I responses to sustained indentation.

II. METHODS

A. Overview

Recordings from *ex vivo* skin-nerve preparations were conducted for six SA-I fibers from five mice using a range of compressive stimuli. Force and firing rate data were analyzed to confirm that firing rates vary significantly from fiber to fiber across a range of forces. Next, a generalized model of the SA-I response was developed in order to better

understand the baseline SA-I response profile, absent fiber-to-fiber variation, and to gain a first approximation of the range of SA-I sensitivities. Finally, force data and the associated coefficients of variation (CV) for inter-spike intervals (ISI) were analyzed to determine if the CVs varied with fiber. Statistical analysis techniques of ANCOVA (Analysis of Covariance) and ANOVA (Analysis of Variance) were used.

B. Experiment

All animal procedures for this experiment were approved by IACUCs of Baylor College of Medicine and the Department of Defense. This experiment involved five wild-type mice, with ages ranging from 3 to 5 months. Of these mice, 1 was male and 5 were female. Hair cycle states were the same for all mice.

From five mice, six skin-nerve preparations were obtained, where saphenous nerve afferents innervating hairy skin were sampled [18]. A segment of nerve was dissected with the hairy skin of the hind paw, which was pinned to a silicone-elastomer substrate (~5 mm thick) in a custom two-compartment organ chamber. The skin was bathed in synthetic interstitial fluid and nerve fibers were teased apart and placed onto an electrode for differential recording. An array of calibrated force fibers was used to locate the receptive field of single afferents and to estimate mechanical thresholds. SA-I responses were distinguished by the following: conduction velocity, $>10 \text{ m}\cdot\text{s}^{-1}$; mechanical threshold, $<1 \text{ mN}$; punctate receptive field, $<0.5 \text{ mm}$ in diameter; slow adaptation; irregular firing pattern; low spontaneous firing rate; and no directional sensitivity to stretch [18-20].

After obtaining a confirmed SA-I afferent, calibrated mechanical displacements were delivered to the punctate receptive field by a custom-built z-stage driven by a linear actuator (Ultra Motion, model D-A.25AB-HT17-2-BR/4). The indenter tip was a macor cylinder 3.0 mm in diameter, similar to the work of Khalsa [16] which imposed forces over the entire SA-I receptive field in order to eliminate stimulus edge effects. The tip was connected to the 1000-g force transducer (Honeywell model 31). The applied force values were measured as a range of displacements was applied. These displacements were chosen on an afferent to afferent basis in order to provide good coverage of the fiber's response range. All indentations reached their target displacements within 75 ms, and were held for 5 s. Across all afferents, displacements ranged from 0.1–2.2 mm and resulted in force magnitudes from 0.00–9.59 mN.

Extracellular recordings were made with a differential amplifier (A-M systems Model 1800) and captured via a DT304 A/D card (Data Translation) and SciWorks Experimenter software (DataWave). Individual action potentials were sorted both online and offline using multidimensional cluster analysis.

C. Data

The dependent measures of firing rate and CV (σ/μ) of inter-spike intervals were calculated from the extracellular recordings, while the independent measure of average force was calculated from the force transducer recordings. All measures were calculated within an analysis window in the slowly adapting portion of the static phase (Fig. 1). This window was 2.5 s in duration and started 2 s after a stimulus reached its final displacement. Double exponential fits were examined to ensure the analysis window was well past the rapidly adapting portion of the SA-I response.

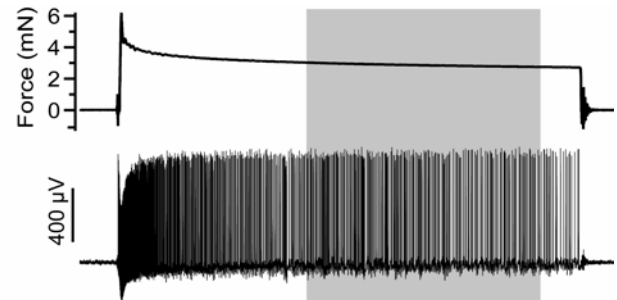


Figure 1: Example trace with 2.5 s analysis window highlighted.

A total of 129 recordings were made, from which force-firing rate pairs were derived. CV-firing rate pairs were similarly derived for the 102 recordings that had responses with three or more spikes (i.e., two or more inter-spike intervals). Additionally, fiber was a factor variable, with each fiber ID a separate level: {A, B, C, D, E, F}. With the exception of D and E, each fiber was from a separate mouse.

D. Statistical Analysis of Firing Rate

As an initial investigation indicated that firing rate was related to force, an ANCOVA was utilized to test the impact of fiber on firing rate. In this ANCOVA, firing rate was the outcome variable, force was the covariate, and the factors of interest were fiber and force-fiber interaction.

E. General Model of Firing Rate

To build a generalized model of firing rate in response to force, the firing rates for each fiber were normalized by dividing all responses from the fiber by the mean of the responses from that fiber. After the data were normalized, curve fitting was used to create a generalized baseline response profile. This baseline response profile, when multiplied by a fiber specific sensitivity factor (mean response for fiber), gives a fiber's response to a force.

F. Statistical Analysis of ISI CV

As an initial investigation indicated that CV was not related to force, an ANOVA was utilized rather than an ANCOVA to test the impact of fiber on CV. In this ANOVA, CV was the outcome variable while fiber was the factor of interest. For this analysis, as well as the statistical analysis of firing rate, we utilized the S-Plus statistical package, Version 8.0. It should be noted that the

insensitivity of ISI CV to force precludes the construction of a model like that developed for firing rate.

III. RESULTS

A. Statistical Analysis of Firing Rate Results

In analyzing the impact of fiber on firing rate, the results indicate that force is a significant covariate, $F(1, 117) = 277.46$, $P < 0.001$, indicating that an ANCOVA analysis is appropriate. Further, fiber was found to be a significant factor, $F(5, 117) = 5.89$, $P < 0.001$, as was force-fiber interaction, $F(5,117) = 6.96$, $P < 0.001$. A graphical comparison of force over fiber (Fig. 2) to firing rate over fiber (Fig. 3) supports this result, as the median firing rate is impacted as much by the fiber as by the median force. For example, the median force for fiber D is less than that of fiber C, yet fiber D exhibits a higher median firing rate than that of fiber C.

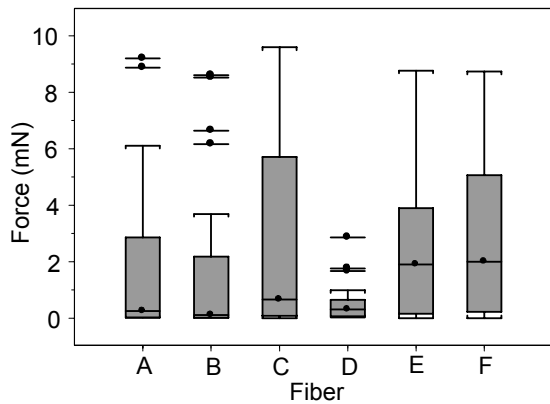


Figure 2: Box plots of force across fibers. Boxes range from lower to upper quartiles, dots within boxes indicate medians, dots outside boxes indicate outliers, and whiskers indicate non-outlier extremes.

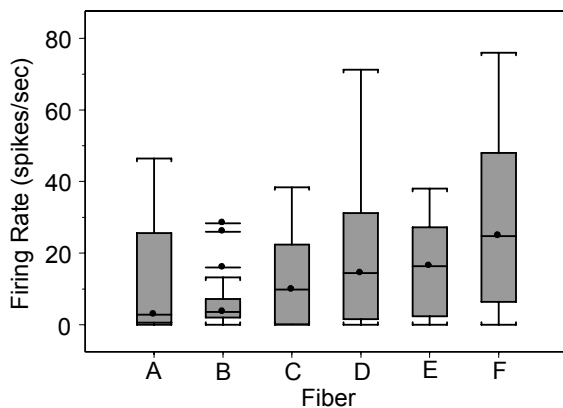


Figure 3: Firing rate across fibers.

B. General Model Results

After normalizing firing rate, the transformation of force to firing rate appears to follow a power function (Eqn. 1) where NR is the normalized response, f is the applied force, and both a and b parameterize the shape of the curve.

$$NR(f) = a * f^b \quad (1)$$

Curve fitting (MATLAB, version 7.7.0) yielded values of $a = 1$ (95% CI: +/- 0.16) and $b = 0.42$ (95% CI: +/- 0.09). These values produce a power function that roughly captures the baseline response profile ($R^2 = 0.62$), although a great deal of variance remains unaccounted for (Fig. 4).

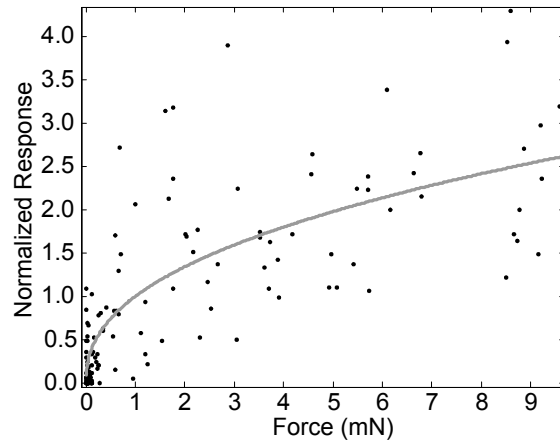


Figure 4: All normalized responses (dots) and baseline response profile obtained through curve fitting and equation 1 (line).

Fiber sensitivity factors obtained during normalization range from 6.61 to 28.58 spikes/s, with fibers A, B, C, D, E, and F having sensitivity factors of 12.04, 6.61, 28.58, 18.26, 15.77, and 13.73 spikes/s, respectively. Therefore, equation 2 describes the generalized model, where r_i is the firing rate for afferent i and S_i is the sensitivity factor for afferent i .

$$r_i(f) = S_i * f^{0.42} \quad (2)$$

C. Statistical Analysis of ISI CV Results

In analyzing the impact of fiber on CV, the results indicate fiber is significant, $F(5, 96) = 3.21$, $P = 0.01$. This result is supported by the graphical examination of CVs over fibers, which shows that median CV differs across fibers from 0.57 to 0.89 (Fig. 5).

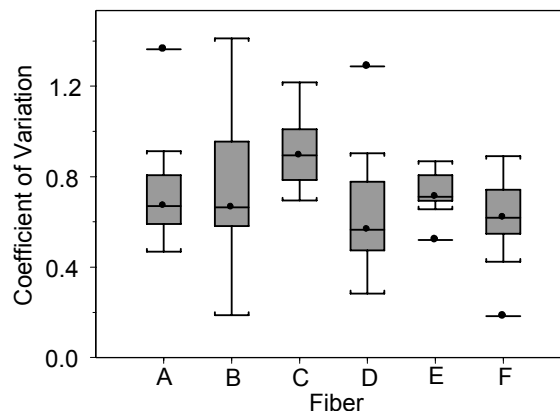


Figure 5: CV across fibers.

IV. DISCUSSION

In this work, we statistically verified that SA-I steady state firing rate varies with fiber. To our knowledge, this work represents the first modeling study of SA-I fibers in a genetically tractable mammal. As noted, there are a number of physiological properties that may explain fiber-to-fiber variation, such as differences in skin stiffness or in the number of Merkel cells in a cluster [11, 21]. The present work lays the groundwork for future studies that will distinguish between these possibilities by using genetic mutations that selectively alter these properties in mice.

Despite the large degree of variation in firing rate from fiber to fiber, firing rate as a function of force could be roughly approximated with a generalized model. This model was in agreement with previous studies where SA-I stimulus-response curves could be approximated by power functions [9, 22] and with studies that have shown that a baseline response profile combined with a fiber specific sensitivity factor yields a general model of the SA-I response [12, 13]. The model may inform the transformation of force sensor data into biologically relevant signals for the emerging class of touch sensitive neural prosthetics [23]. Additionally, as similar models have been aggregated into population models for investigating the effects of innervation density and distribution on the discrimination of objects [12, 13], the model may be aggregated into simulations for optimizing sensor distributions within tactile prosthetics.

Even when normalizing to account for fiber specific sensitivities, the variability of steady state responses is quite high. This may indicate that a large degree of variability is acceptable, or possibly beneficial, in systems providing artificial tactile feedback. For example, under certain circumstances, the addition of noise in a sensory system can actually increase the signal to noise ratio through stochastic resonance [24]. However, this requires further investigation and the work described here only provides an initial indication of how much variability is acceptable.

In addition to analyzing and modeling firing rate, this work also demonstrated that the CV of inter-spike intervals varies with fiber. This variation may be explained by the number of Merkel cells in a cluster [11]. Additional studies, however, are required to investigate this possibility.

REFERENCES

- [1] J. R. Phillips and K. O. Johnson, "Tactile Spatial Resolution. II. Neural Representation of Bars, Edges, and Gratings in Monkey Primary Afferents," *Journal of Neurophysiology*, vol. 46, pp. 1192-1203, 1981.
- [2] A. Iggo and A. R. Muir, "The structure and function of a slowly adapting touch corpuscle in hairy skin," *J Physiol*, vol. 200, pp. 763-796, 1969.
- [3] R. S. Johansson, U. Lundström, and R. Lundström, "Sensitivity to edges of mechanoreceptive afferent units innervating the glabrous skin of the human hand," *Brain Research*, vol. 244, pp. 27-32, 1982.
- [4] M. Paré, H. Carnahan, and A. Smith, "Magnitude estimation of tangential force applied to the fingerpad," *Experimental Brain Research*, vol. 142, pp. 342-348, 2002.
- [5] R. S. Johansson, "Tactile sensibility in the human hand: receptive field characteristics of mechanoreceptive units in the glabrous skin area," *J Physiol*, vol. 281, pp. 101-125, 1978.
- [6] E. A. Lumpkin, T. Collisson, P. Parab, A. Omer-Abdalla, H. Haeberle, P. Chen, A. Doetzelhofer, P. White, A. Groves, N. Segil, and J. E. Johnson, "Math1-driven GFP expression in the developing nervous system of transgenic mice," *Gene Expr Patterns*, vol. 3, pp. 389-95, 2003.
- [7] D. Guinard, Y. Usson, C. Guillermet, and R. Saxod, "Merkel complexes of human digital skin: three-dimensional imaging with confocal laser microscopy and double immunofluorescence," *J Comp Neurol*, vol. 398, pp. 98-104, 1998.
- [8] Z. Halata, M. Grim, and K. I. Baumann, "[The Merkel cell: morphology, developmental origin, function]," *Cas Lek Cesk*, vol. 142, pp. 4-9, 2003.
- [9] M. Knibestol, "Stimulus-response functions of slowly adapting mechanoreceptors in the human glabrous skin area," *J Physiol*, vol. 245, pp. 63-80, 1975.
- [10] U. Proske, "Irregularity in the discharge of slowly adapting mechanoreceptors," in *Studies in Neurophysiology: Presented to A.K. McIntyre*, R. Porter, Ed. Cambridge: University Press, 1978, pp. 87-98.
- [11] K. W. Horch, D. Whitehorn, and P. R. Burgess, "Impulse generation in type I cutaneous mechanoreceptors," *J Neurophysiol*, vol. 37, pp. 267-281, 1974.
- [12] A. W. Goodwin and H. E. Wheat, "Effects of Nonuniform Fiber Sensitivity, Innervation Geometry, and Noise on Information Relayed by a Population of Slowly Adapting Type I Primary Afferents from the Fingerpad," *J. Neurosci.*, vol. 19, pp. 8057-8070, 1999.
- [13] A. W. Goodwin and H. E. Wheat, "How is tactile information affected by parameters of the population such as non-uniform fiber sensitivity, innervation geometry and response variability?," *Behav Brain Res*, vol. 135, pp. 5-10, 2002.
- [14] A. W. Freeman and K. O. Johnson, "Cutaneous Mechanoreceptors in Macaque Monkey - Temporal Discharge Patterns Evoked by Vibration, and a Receptor Model," *Journal of Physiology-London*, vol. 323, pp. 21-41, 1982.
- [15] F. J. Looft, "Response of monkey glabrous skin mechanoreceptors to random-noise sequences: I. Temporal response characteristics," *Somatosen Mot Res*, vol. 11, pp. 327-44, 1994.
- [16] W. Ge and P. S. Khalsa, "Encoding of Compressive Stress During Indentation by Slowly Adapting Type I Mechanoreceptors in Rat Hairy Skin," *J Neurophysiol*, vol. 87, pp. 1686-1693, 2002.
- [17] H. Burton and R. J. Sinclair, "Attending to and remembering tactile stimuli: a review of brain imaging data and single-neuron responses," *J Clin Neurophysiol*, vol. 17, pp. 575-91, 2000.
- [18] M. Koltzenburg, C. L. Stucky, and G. R. Lewin, "Receptive Properties of Mouse Sensory Neurons Innervating Hairy Skin," *J Neurophysiol*, vol. 78, pp. 1841-1850, 1997.
- [19] P. W. Reeh, "Sensory receptors in mammalian skin in an in vitro preparation," *Neurosci Lett*, vol. 66, pp. 141-6, 1986.
- [20] D. M. Cain, S. G. Khasabov, and D. A. Simone, "Response properties of mechanoreceptors and nociceptors in mouse glabrous skin: an in vivo study," *J Neurophysiol*, vol. 85, pp. 1561-74, 2001.
- [21] M. A. Serrat, C. I. Vinyard, and D. King, "Alterations in the mechanical properties and composition of skin in human growth hormone transgenic mice," *Connective Tissue Research*, vol. 48, pp. 19-26, 2007.
- [22] G. Werner and V. B. Mountcastle, "Neural Activity in Mechanoreceptive Cutaneous Afferents: Stimulus-Response Relations, Weber Functions, and Information Transmission," *J Neurophysiol*, vol. 28, pp. 359-97, 1965.
- [23] G. S. Dhillon and K. W. Horch, "Direct neural sensory feedback and control of a prosthetic arm," *IEEE Trans Neural Syst Rehabil Eng*, vol. 13, pp. 468-72, 2005.
- [24] F. Moss, L. M. Ward, and W. G. Sannita, "Stochastic resonance and sensory information processing: a tutorial and review of application," *Clin Neurophysiol*, vol. 115, pp. 267-81, 2004.